Observation of high-temperature spin-freezing behavior in $Cd_{1-x-y}Mn_xFe_yTe$

Y. Irie and T. Sato
Department of Instrumentation Engineering, Faculty of Science and Technology, Keio University, 3-14-1 Hiyoshi, Kohoku-ku, Yokohama-shi, Kanagawa, Japan

E. Ohta
Department of Materials Science, Faculty of Science and Technology, Keio University, 3-14-1 Hiyoshi, Kohoku-ku, Yokohama-shi, Kanagawa, Japan

(Received 30 November 1994)

The temperature-dependent magnetic susceptibility of single-crystal $Cd_{1-x-y}Mn_xFe_yTe$ ($x=0.26, 0.30, 0.37, 0.44, 0.58$; $y\sim0.01$) showed that the cusp temperature T_g is higher than that of $Cd_{1-x}Mn_xTe$ with the same Mn content. This is ascribed to the stronger Mn-Mn interaction, which is caused by a decrease in the lattice constant accompanied with doping of the Fe into $Cd_{1-x}Mn_xTe$. We scarcely observed the intrinsic difference between $Cd_{1-x-y}Mn_xFe_yTe$ and $Cd_{1-x}Mn_xTe$ samples except for $Cd_{0.62}Mn_{0.37}Fe_{0.01}Te$, which shows quite a peculiar magnetic behavior. The temperature-dependent magnetic susceptibility of $Cd_{0.62}Mn_{0.37}Fe_{0.01}Te$ at temperatures above T_g shows a minimum around 100 K and increases as the temperature further increases and the thermal hysteresis still remains up to 340 K. The time-dependent remanent magnetization of $Cd_{0.62}Mn_{0.37}Fe_{0.01}Te$ suggests a spin-glass-like relaxation retained even at $T\sim250$ K. Such high-temperature spin-freezing behavior can be interpreted in terms of the bound magnetic polaron formation with a carrier localization.

I. INTRODUCTION

Many intensive studies have been done on Mn-based II-VI diluted magnetic semiconductors (DMS), $A^{II}_{1-x}Mn_xB^{VI}$, because of their interesting properties. Examples include the giant Faraday rotation, spin-glass behavior, photo luminescence dominated by exciton-magnetic polaron complexes and so on.[1] Such characteristics of the Mn-based DMS are mainly caused by two types of exchange interactions. One type is the *sp-d* exchange interaction between the band electron spins and the localized moments of the magnetic ions, which has a significant influence on the optical and electrical properties. Another is the super-exchange (*d-d* exchange) interaction between the localized magnetic ions, which is mainly responsible for the magnetic properties. Recent investigations of the Fe-based DMS, $A^{II}_{1-x}Fe_xB^{VI}$,[2,3] showed that the magnetic behavior is different from the Mn-based system, which originates from the fact that the Fe^{2+} ions possess both spin and orbital momenta ($S=2$, $L=2$) whereas Mn^{2+} ions possess only spin momentum ($S=\frac{5}{2}$). Mn-based DMS shows a Curie-type paramagnetism contrast to the typical Van Vleck-type paramagnetism[4] of the Fe-based DMS.

So far, we have intended to characterize the low-temperature spin-freezing state in $Cd_{1-x}Mn_xTe$ by the nonlinear susceptibility[5] and the magnetic relaxation process.[6] Although the spin-glass-like behavior of $Cd_{1-x}Mn_xTe$ is ascribed to the antiferromagnetic interaction between the localized Mn moments,[7] it is still an open question whether it is identified to the spin glass or antiferromagnetic cluster freezing. This ambiguity of the spin-freezing mechanism partly originates from the lack of the magnetic information on the microscopic scale due to difficulty of the neutron-scattering study. It must be useful to modify the local magnetic environment by doping extrinsic impurity into $Cd_{1-x}Mn_xTe$ to specify the magnetic origin of the spin freezing. Therefore, we have investigated the magnetic properties of $Cd_{1-x-y}Mn_xFe_yTe$ in which the interaction is disturbed by replacing some Mn ions with Fe ions, since the Fe ion in $Cd_{1-x}Mn_xTe$ is expected to be magnetically inactive. Thus, we have reported the magnetic properties of the Fe-doped Mn-based DMS, $Cd_{1-x-y}Mn_xFe_yTe$ ($y\sim0.01$) compared with the spin freezing of $Cd_{1-x}Mn_xTe$.

II. EXPERIMENT

We decided to select the Fe concentration of $y=0.01$ to prepare the $Cd_{1-x-y}Mn_xFe_yTe$ samples, since the zinc-blende-type structure of $Cd_{1-x}Fe_xTe$ is realized within 6-at. % Fe and the good quality single crystal can be obtained less than only 1 at. %.[8] A mixture of CdTe, MnTe, Fe, and Te was encapsulated in a carbon-coated quartz ampule according to the desirable Mn and Fe concentrations. It was annealed at 1100° C for 12 h, and the polycrystalline $Cd_{1-x-y}Mn_xFe_yTe$ was obtained. Then, the single crystals of $Cd_{1-x-y}Mn_xFe_yTe$ were prepared using the Bridgman technique. The composition and homogeneity of the prepared samples were evaluated by an electron probe microanalyzer (EPMA). The crystal structure of the sample was examined by the x-ray diffraction method. The structure of the prepared $Cd_{1-x-y}Mn_xFe_yTe$ single crystals, with Mn and Fe concentrations as shown in Table I, is verified to be the zinc-blende type, identical to that of $Cd_{1-x}Mn_xTe$. The lattice constants linearly depends on the Mn content as is shown in Fig. 1 and is smaller than that of $Cd_{1-x}Mn_xTe$

TABLE I. Mn concentration for single crystal $Cd_{1-x-y}Mn_xFe_yTe$ ($y \sim 0.01$) samples, which were determined by EPMA.

Sample No.	Mn concentration x
0	0.37
1	0.43
2	0.58
4	0.26
5	0.30
6	0.37

with the same Mn content, which is derived from the Vegard's law reported by Furdyna *et al.*[9]

The magnetic measurement was performed using a superconducting quantum interference device magnetometer (Quantum Design MPMS-5). The temperature-dependent magnetic susceptibility was measured between 6 and 400 K under the zero-field-cooled (ZFC) and field-cooled (FC) conditions. The time-dependent thermoremanent magnetization (TRM) was measured according to the following procedure. A sample was cooled down from 400 K to a desired temperature in the external magnetic field H_{cool}. The field was turned off after waiting for about 100 sec, and then we started to measure the remanent magnetization as a function of time. The origin of time $t=0$, was defined as the moment when the exciting current in the superconducting solenoid attains to zero. The electrical resistivity was measured using the Van der Pauw technique at room temperature.

III. EXPERIMENTAL RESULTS

The temperature-dependent magnetic susceptibility of $Cd_{1-x-y}Mn_xFe_yTe$ with $x=0.26$, 0.30, 0.44, 0.58, and $y=0.01$ is similar to that of $Cd_{1-x}Mn_xTe$ as follows. The ZFC susceptibility shows a cusp at low temperatures and the thermal hysteresis is observed below the cusp temperature T_g; the Curie-type paramagnetism is recognized above T_g (Fig. 2). Figure 2 also shows that the magnetic susceptibility per Mn mole of $Cd_{1-x-y}Mn_xFe_yTe$ decreases with increasing Mn concentration, which is same as that of $Cd_{1-x}Mn_xTe$. Such Mn concentration dependence of the magnetic moment must originate from the antiferromagnetic interaction between Mn moments, which increases with increasing Mn content. On the other hand, $Cd_{0.62}Mn_{0.37}Fe_{0.01}Te$ shows the peculiar magnetic behavior, i.e, the temperature-dependent magnetic susceptibility in 100 Oe above T_g ($=13.5$ K) shows a minimum around 100 K, and increases as the temperature further increases, and the thermal hysteresis still remains up to 340 K (Fig. 3). Moreover the magnetic susceptibility of $Cd_{0.62}Mn_{0.37}Fe_{0.01}Te$ is tenfold larger than that of $Cd_{1-x}Mn_xTe$ with the same Mn content. Such a feature can be observed only in the magnetic fields below 500 Oe.

The cusp temperatures T_g of $Cd_{1-x-y}Mn_xFe_yTe$ are shown in Fig. 4 as a function of the Mn content in comparison with those of $Cd_{1-x}Mn_xTe$, which are derived from the phase diagram reported by Oseroff *et al.*[1] The cusp temperature of $Cd_{1-x-y}Mn_xFe_yTe$ is higher than that of $Cd_{1-x}Mn_xTe$ with the same Mn content. Here, we should note that there is no anomalous behavior in Fig. 4 around $x=0.37$. On the basis of Figs. 1 and 4, the relation between T_g and the lattice constants is derived as shown in Fig. 5. We note that the cusp temperature of $Cd_{1-x-y}Mn_xFe_yTe$ is equal to that of $Cd_{1-x}Mn_xTe$ with the same lattice constant down to 6.423 Å, which corresponds to the Mn concentration $x=0.43$ of

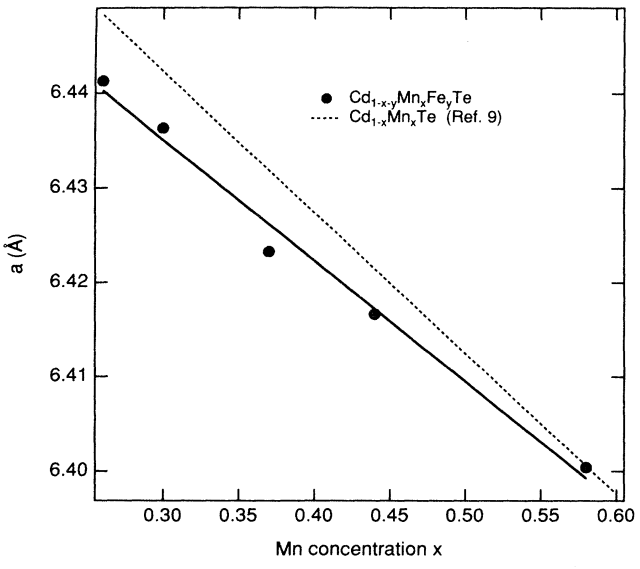

FIG. 1. Mn concentration-dependent lattice constant of $Cd_{1-x-y}Mn_xFe_yTe$. The broken line represents the lattice constants of $Cd_{1-x}Mn_xTe$ according to the Vegard's law proposed in Ref. 9.

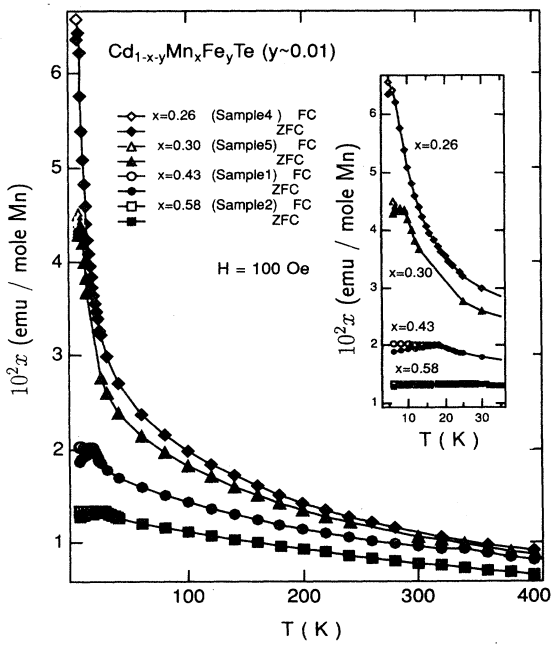

FIG. 2. Temperature-dependent magnetic susceptibility of $Cd_{1-x-y}Mn_xFe_yTe$ ($x=0.26$, 0.30, 0.43, 0.58, and $y \sim 0.01$).

$Cd_{1-x}Mn_xTe$. For the small lattice constant below 6.432 Å, T_g of $Cd_{1-x-y}Mn_xFe_yTe$ shows a larger increment than that of $Cd_{1-x}Mn_xTe$ with a decreasing lattice constant.

The magnetic susceptibility of $Cd_{1-x-y}Mn_xFe_yTe$ can be fitted with the Curie-Weiss law after subtracting the diamagnetic susceptibility of the host CdTe.[10] The Curie constant and the Curie temperature are shown as a function of Mn concentration in Figs. 6 and 7 with those of $Cd_{1-x}Mn_xTe$, which are reported by Oseroff,[11] where the values for $Cd_{0.62}Mn_{0.37}Fe_{0.01}Te$ are derived from the paramagnetic component mentioned in Sec. IV. We scarcely detected essential changes in the Curie temperature with the doping Fe atom, while the Curie constant is larger than that of $Cd_{1-x}Mn_xTe$.

The TRM of $Cd_{1-x-y}Mn_xFe_yTe$ depends on time at temperatures below T_g, which is intrinsically the same as that of $Cd_{1-x}Mn_xTe$. On the other hand, the time-dependent TRM of $Cd_{0.62}Mn_{0.37}Fe_{0.01}Te$ was also observed at several temperatures higher than T_g as shown in Fig. 8 where the FC procedure is performed in

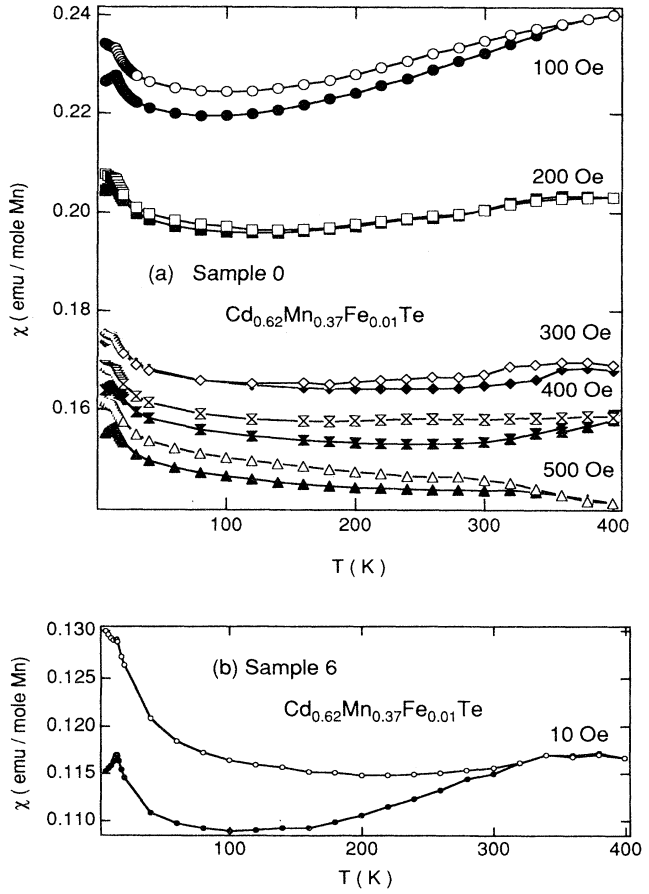

FIG. 3. Temperature-dependent magnetic susceptibility of $Cd_{0.62}Mn_{0.37}Fe_{0.01}Te$ (sample 0) in several magnetic fields (a). The other $x=0.37$ sample (sample 6) shows the similar temperature dependence to the sample 0 (b). The closed symbols represent the ZFC condition and the open symbols represent the FC condition in (a) and (b).

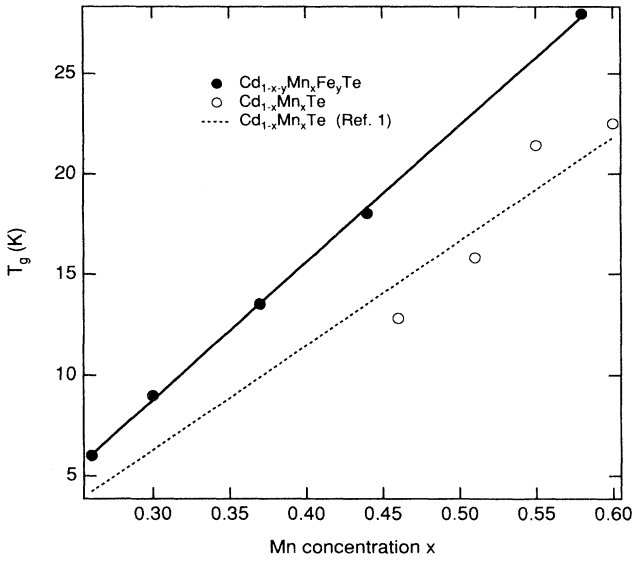

FIG. 4. Mn concentration-dependent cusp temperatures of $Cd_{1-x-y}Mn_xFe_yTe$ and $Cd_{1-x}Mn_xTe$. The closed circle represents the data for $Cd_{1-x-y}Mn_xFe_yTe$. The open circle represents that of $Cd_{1-x}Mn_xTe$ obtained from our previous paper (Ref. 6). The cusp temperature of $Cd_{1-x}Mn_xTe$ quoted from the phase diagram in Ref. 1 is represented by the broken line.

$H_{cool}=100$ Oe. Namely, the thermal evolution of TRM of $Cd_{0.62}Mn_{0.37}Fe_{0.01}Te$ is abridged as follows. The long-time decay of TRM observed at low temperatures [Fig. 8(a)] once vanishes at 20 K [Fig. 8(b)]. It appears again at 150 K [Fig. 8(e)] and grows up to 250 K [Figs. 8(f) and 8(g)]. Then, it fades out at 300 K [Fig. 8(h)]. At the whole temperatures, the time-dependent TRM can be

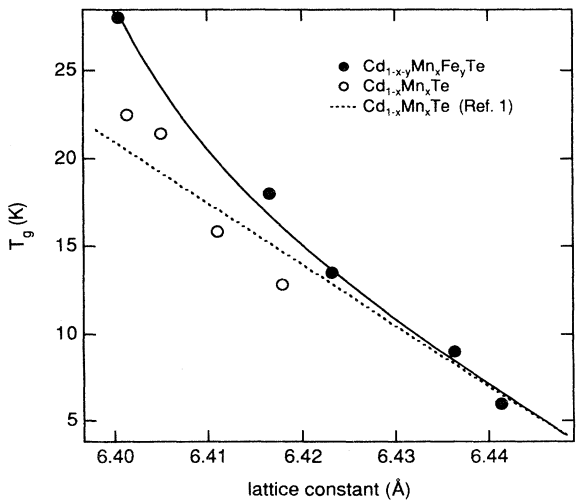

FIG. 5. Lattice-constant-dependent cusp temperature of $Cd_{1-x-y}Mn_xFe_yTe$ and $Cd_{1-x}Mn_xTe$. The lattice-constant-dependent cusp temperature derived from Refs. 1 and 9 is represented by the broken line. The solid line is a guide for the eyes.

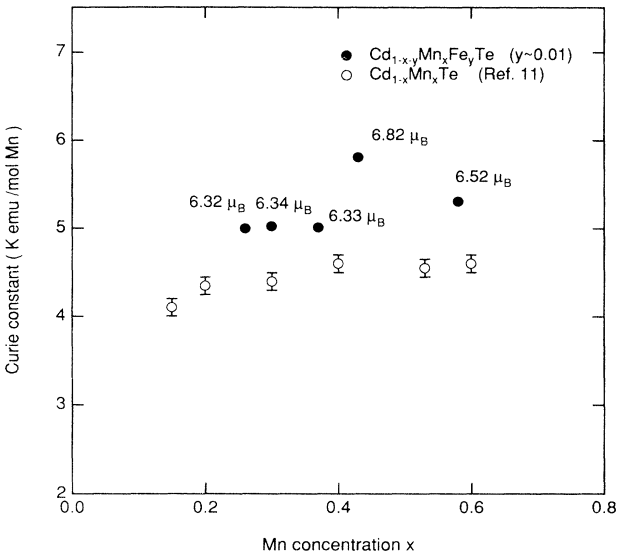

FIG. 6. Mn concentration-dependent Curie constants of $Cd_{1-x-y}Mn_xFe_yTe$. The values of magnetic moments derived from the Curie constants are also shown in this figure. The data for $Cd_{1-x}Mn_xTe$ are quoted from Ref. 11.

fitted with the power law

$$TRM = At^{-n}, \quad (1)$$

which is supported by $\log_{10}$ (TRM) vs $\log_{10}t$ plot as shown in Fig. 9(a). As shown in Fig. 9(b), the temperature-dependent exponent n, determined by the least-squares method, well reflects the temperature-dependent feature of magnetization relaxation described above. Such long-time decay of TRM at higher temperatures is suggestive of the spin-glass-like relaxation, while it disappears when the FC procedure is performed in a field above 500 Oe at which the peculiarity in magnetic susceptibility of $Cd_{0.62}Mn_{0.37}Fe_{0.01}Te$ also becomes indistinct (Fig. 3).

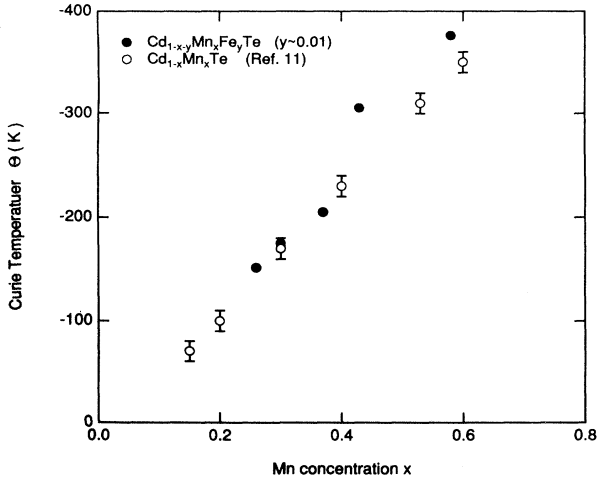

FIG. 7. Mn concentration-dependent Curie temperatures of $Cd_{1-x-y}Mn_xFe_yTe$. The data for $Cd_{1-x}Mn_xTe$ are quoted from Ref. 11.

The electrical resistivity of $Cd_{1-x-y}Mn_xFe_yTe$ at room temperature shows a maximum at Mn concentrations $x = 0.37$. Here, we should note that such a maximum was also reported in $Cd_{1-x}Mn_xTe$ at $x = 0.4$ by Triboulet and Didier[12] (Fig. 10). The electrical resistivity of $Cd_{1-x-y}Mn_xFe_yTe$ with $x < 0.37$ is higher than that of $Cd_{1-x}Mn_xTe$ with the same Mn content, which is contrary to the relation for $x > 0.37$. Thus, the electrical resistivity of $Cd_{1-x-y}Mn_xFe_yTe$ shows a singular behavior around the Mn concentration at which the magnetic susceptibility shows the peculiar temperature dependence. Such a correlation between the magnetic and electrical properties must give some important information to specify the magnetic contribution resulting from the doping of Fe into $Cd_{1-x}Mn_xTe$.

IV. DISCUSSION

We can classify the Mn concentration of $Cd_{1-x-y}Mn_xFe_yTe$ into the following three regions based on the magnetic behavior and the electrical resis-

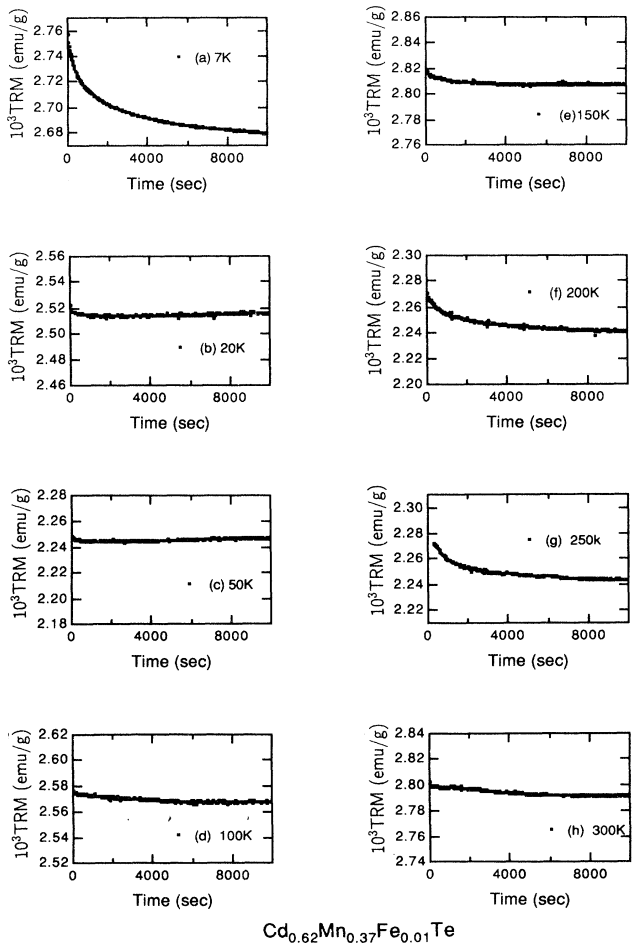

FIG. 8. Time-dependent thermoremanent magnetization of $Cd_{0.62}Mn_{0.37}Fe_{0.01}Te$. All sales in the axis of ordinates are identical in the figures.

tivity at room temperature. For $x<0.37$, the cusp temperature shows the common increment with decreasing the lattice constant between $Cd_{1-x-y}Mn_xFe_yTe$ and $Cd_{1-x}Mn_xTe$. At $x=0.37$, we observed some peculiar magnetic behavior mentioned above and the singular high electrical resistivity. When the Mn content exceeds $x=0.37$, the cusp temperature of $Cd_{1-x-y}Mn_xFe_yTe$ shows larger increments than that of $Cd_{1-x}Mn_xTe$ as a function of the lattice constant and the electrical resistivity steeply decreases. Thus, we will separately discuss the magnetic nature of $Cd_{1-x-y}Mn_xFe_yTe$ in these Mn concentration regions in the following paragraph.

A. The spin-glass state of $Cd_{1-x-y}Mn_xFe_yTe$ samples ($x<0.37$)

The cusp temperatures of $Cd_{1-x-y}Mn_xFe_yTe$ and $Cd_{1-x}Mn_xTe$ are scaled with the lattice constant in this region. In other words, the change in lattice constant, explained by the fact that $Cd_{1-x}Fe_xTe$ has a smaller lattice constant compared with $Cd_{1-x}Mn_xTe$,[8,9] mainly characterizes the magnetic nature in $Cd_{1-x-y}Mn_xFe_yTe$ as the contribution of Fe doping. This scaling behavior indicates that the Mn-Mn magnetic interaction sensitive to the atomic distance determines the cusp temperature of $Cd_{1-x-y}Mn_xFe_yTe$ and $Cd_{1-x}Mn_xTe$ in the lower Mn concentration region, which is consistent with the spin-glass picture expected for the dilute magnetic $Cd_{1-x}Mn_xTe$. The other detectable contribution of the Fe dopant is the increase in the Curie constant of $Cd_{1-x-y}Mn_xFe_yTe$, which is observed over the whole Mn concentration region. The origin of this feature can be explained in terms of the magnetic polarization of s and p electrons[13] and/or the bound-magnetic-polaron (BMP) formation[14,15] when they are enhanced by the Fe doping. However, these contributions scarcely bring about any intrinsic changes in the magnetic nature in this Mn concentration region.

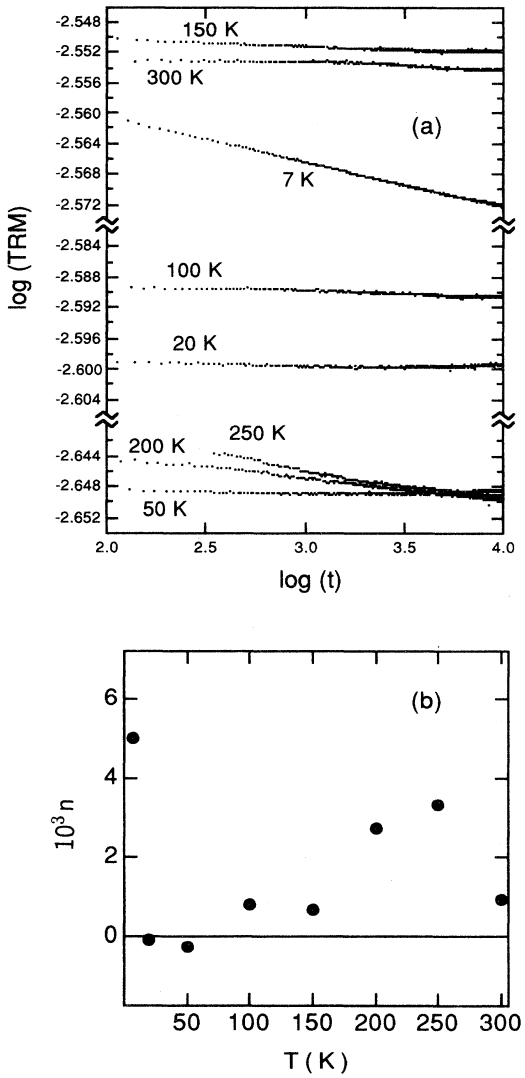

FIG. 9. Double logarithmic plot (to base 10) of TRM vs time (a). Temperature dependence of the exponent n in Eq. (1) of $Cd_{0.62}Mn_{0.37}Fe_{0.01}Te$.

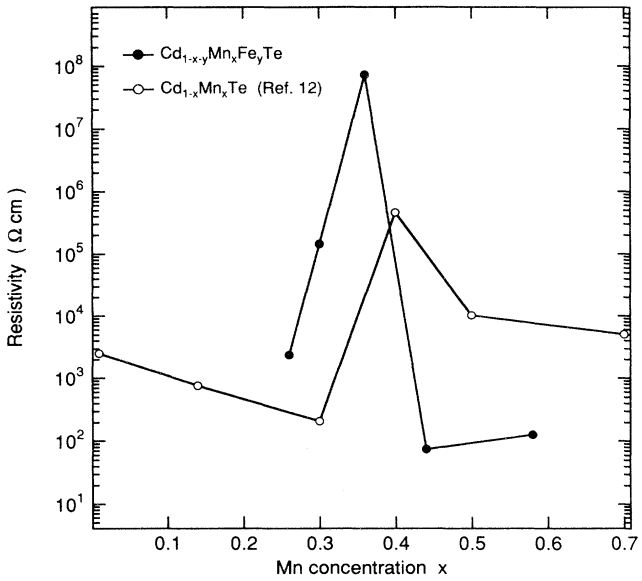

FIG. 10. Electrical resistivity of $Cd_{1-x-y}Mn_xFe_yTe$ at room temperature shown as a function of the Mn concentration. The data for $Cd_{1-x}Mn_xTe$ are quoted from Ref. 12.

B. Appearances of the high-temperature spin-freezing behavior at the $x=0.37$ sample

The characteristics observed in $Cd_{0.62}Mn_{0.37}Fe_{0.01}Te$ is abridged as follows: (1) the tenfold larger magnetic susceptibility than that of $Cd_{1-x}Mn_xTe$ with same Mn content, (2) the increase in magnetic susceptibility with increasing temperatures observed at temperatures much higher than the cusp temperature, (3) the reappearance of the long-time decay of TRM in the temperature region, where the peculiar increase in the magnetic susceptibility is observed, and (4) the singular high electrical resistivity at room temperature. Prior to the specification of the magnetic nature in the $x=0.37$ sample, we must mention that these characteristic behaviors were reconfirmed in

the other samples with $x \sim 0.37$ as shown in Fig. 3(b) and restricted in the narrow Mn concentration region at around $x = 0.37$. This denies any possible contribution from the magnetic contamination due to some mixture such as Fe, FeTe, and $FeTe_2$, which may have happened during the sample preparation process.

First, we paid attention to our previous study on the magnetization curve of $Cd_{0.62}Mn_{0.37}Fe_{0.01}Te$, where the magnetization process consisted of two magnetic contributions, i.e., the ferromagnetic and paramagnetic components.[16] The separation of these magnetic contributions can be attained under both the FC and ZFC conditions. Recently, Ohno *et al.* reported such coexistence of these contributions in the dilute magnetic III-V semiconductor (In, Mn)As.[17] They showed that the ferromagnetic component that appeared at a low temperature brings out a steep increase in the electrical resistivity, and the origin was explained in terms of a large BMP formation accompanied by the carrier localization. Such a picture may give some feasible explanation for the peculiar magnetic behavior in our present sample. Thus, we tried to discuss a possible mechanism of BMP formation in $Cd_{1-x-y}Mn_xFe_yTe$. The optical measurements have given us some evidence for the magnetic polaron forming in $Cd_{1-x}Mn_xTe$, which causes the locally aligned Mn spins continuing during several picoseconds,[18] whereas the static magnetic behavior relevant to it has been scarcely investigated. Provided that the magnetic polaron is bound at the Fe dopant in $Cd_{1-x-y}Mn_xFe_yTe$, we can expect that the magnetic contribution due to the polarized Mn spins is enhanced via the polarization of the valence electrons due to the Fe atom. Such an idea is partly supported by the fact that the Fe doping brings an increase in the Curie constant. Furthermore, the singular high electrical resistivity at $x = 0.37$ reflects one of the most remarkable characteristics expected in the BMP formation, i.e., the increase in the effective mass of the conduction electrons. Thus, we have obtained some evidence supporting the BMP formation in $Cd_{0.62}Mn_{0.37}Fe_{0.01}Te$. The lower electrical resistivity in the Mn concentration with $x < 0.37$ suggests a weak localization of the conduction of electrons due to the weakly polarized field and/or the diminishing of polaron formation.

The peculiar temperature dependence of the magnetic behavior must be also explained in terms of the BMP formation. Here, we introduce the idea of the interactive magnetic polarons so as to bring about the long-time magnetic relaxation as observed in $Cd_{0.62}Mn_{0.37}Fe_{0.01}Te$. Thus, this mechanism coexists with the Mn-Mn antiferromagnetic interaction, which should be the origin of the low-temperature spin-freezing behavior that is commonly observed in the wide Mn concentration region. These two types of magnetic interactions enable the following explanation for the temperature-dependent magnetic behavior in the $x = 0.37$ sample. Below the cusp temperature, the Mn-Mn antiferromagnetic interaction is so strong that the formation of the BMP must be disturbed. Thus, the spin-freezing nature at low temperatures is essentially the same as that in the lower Mn concentration regions. As the antiferromagnetic interaction becomes weaker, with increasing temperature, the aligned Mn spins appears due to the growth of the BMP, which modifies the Curie-type decrease in magnetic susceptibility. When the size of the BMP further grows up, the inevitable interaction between the BMP's must bring about the reincrease in the magnetic susceptibility with the thermal irreversible behavior and the long-time relaxation of magnetization. Such high-temperature spin-freezing behavior should be sensitive to magnitude of the magnetic field, since the Mn moment begins to align in a comparative low external field so that the BMP would become unstable. This picture is also consistent with the disappearance of the reincrease of the magnetic susceptibility in fields above 500 Oe. Thus, we believe that the appearance of the high-temperature spin-freezing behavior in $Cd_{0.62}Mn_{0.37}Fe_{0.01}Te$ should be mainly interpreted based on the BMP formation.

C. The magnetic cluster formation in the Mn concentrated $Cd_{1-x-y}Mn_xFe_yTe$ samples ($x > 0.37$)

The scaling of the cusp temperature with the lattice constant is failed in the Mn concentrated $Cd_{1-x-y}Mn_xFe_yTe$ samples with $x > 0.37$. This suggests an intrinsic change in the local magnetic environment, which is responsible for the more frustrated magnetic nature compared with that observed for the lower Mn concentration. Here, we should note that the corresponding Mn concentration $x = 0.43$ in $Cd_{1-x}Mn_xTe$ having the same lattice constant as $Cd_{0.62}Mn_{0.37}Fe_{0.01}Te$ is very close to the critical Mn concentration $x_c = 0.46$ at which the freezing of antiferromagnetic clusters replaces the spin-glass freezing.[5,6] Provided that the Fe dopant encourages such a cluster formation in $Cd_{1-x-y}Mn_xFe_yTe$, the low-temperature magnetic behavior for $x > 0.37$ can contain the contribution from the intercluster freezing. The cluster formation should cause the increase in the cusp temperature with doping Fe atoms. Furthermore, the rapid decrease in the electrical resistivity above $x = 0.37$ may cause a long-range Mn-Mn interaction via the conduction electrons, which can be also responsible for the failure in the lattice constant scaling. As we expected such stronger Mn-Mn interaction realized in the sample with $x > 0.37$, BMP becomes difficult to be formed in this Mn concentration region. Thus, the occurrence of a peculiar magnetic behavior due to the BMP formation must be restricted to the narrow Mn concentration around $x = 0.37$.

V. CONCLUSION

The magnetic nature of $Cd_{1-x-y}Mn_xFe_yTe$ was characterized separately in the three Mn concentration regions with $x < 0.37$, $x = 0.37$, and $x > 0.37$. The lower Mn concentration sample has essentially the same spin-glass nature as $Cd_{1-x}Mn_xTe$. The $x = 0.37$ sample shows the high-temperature spin-freezing behavior interpreted in terms of the bound magnetic polaron formation in addition to the low-temperature spin-glass nature that

is common to the lower Mn concentration samples. The Mn concentrated sample is characterized with the cluster freezing process rather than the BMP formation. We believe that the BMP formation is the key to interpreting the magnetic nature of $Cd_{1-x-y}Mn_xFe_yTe$, especially to the high-temperature spin-glass-like freezing in $Cd_{0.62}Mn_{0.37}Fe_{0.01}Te$, which can be explained only by introducing the mechanism based on it. We are planning to measure the Mössbauer spectroscopy to obtain a detailed picture of the high spin-freezing behavior.

ACKNOWLEDGMENT

We wish to thank Mr. N. Takaya and Mr. S. Ohta for their help with the discussion and sample preparation. This work was partially supported under the Grant-in-Aid for Science Research from the Ministry of Education, Science and Culture, by the Asahi Glass Foundation, Kanagawa Academy of Science and Technology Foundation, Saneyoshi Scholarship Foundation, and Mazda Foundation's Research Grant.

[1]S. B. Oseroff, in *Diluted Magnetic Semiconductors,* edited by J. K. Furdyna and K. Kossut, Semiconductors and Semimetals Vol. 25 (Academic, New York, 1988).

[2]A. Lewicki, J. Spalek, and A. Mycielski, J. Phys. C **20**, 2005 (1987).

[3]A. Sarem, B. J. Kowalski, and B. A. Orloski, J. Phys. Condens. Matter **2**, 8173 (1990).

[4]E. Kartheuser, S. Rodriguez, and M. Villeret, Phys. Rev. B **48**, 14 127 (1993).

[5]Y. Irie, K. Jochi, T. Sato, and E. Ohta, Jpn. J. Appl. Phys. **32**, 410 (1993).

[6]Y. Irie, K. Jochi, T. Sato, and E. Ohta, Jpn. J. Appl. Phys. **32**, 414 (1993).

[7]N. B. Brandt and V. V. Moshchalkov, Adv. Phys. **33**, 193 (1984).

[8]A. Sarem, B. J. Kowalski, J. Majewski, J. Górecka, B. A. Orlowski, A. Mycielski, and K. Jezierski, Acta Phys. Pol. **2-3**, 407 (1990).

[9]J. K. Furdyna, W. Griat, D. F. Mitchell, and G. I. Sproule, J. Solid State Chem. **46**, 349 (1983).

[10]R. M. Candea, S. J. Hudgens, and M. Kastner, Phys. Rev. B **18**, 2733 (1978).

[11]S. B. Oseroff, Phys. Rev. B **25**, 6584 (1982).

[12]R. Triboulet and G. Didier, J. Cryst. Growth **52**, 614 (1981).

[13]M. H. Tsai, J. D. Dow, R. V. Kasowski, A. Wall, and A. Franciosi, Solid State Commun. **69**, 1131 (1989).

[14]P. A. Wolff and J. Warnock, J. Appl. Phys. **55**, 2300 (1984).

[15]R. N. Kershaw, D. Ridgley, K. Dwight, A. Wold, R. R. Galazka, and W. Giriat, Phys. Rev. B **35**, 6950 (1987).

[16]Y. Irie, T. Sato, and E. Ohta, J. Magn. Magn. Mater. **140-144**, 2027 (1995).

[17]H. Ohno, H. Munekata, T. Penny, S. von Molnár, and L. L. Chang, Phys. Rev. Lett. **68**, 2664 (1992).

[18]Y. Oka, K. Nakamura, I. Souma, M. Kido, and H. Fujisaki, J. Lumin. **38**, 263 (1987).